Determination of Artesunate by Capillary Electrophoresis with Low UV Detection and Possible Applications to Analogues

A. D'Hulst, P. Augustijns*, S. Arens, L. Van Parijs, S. Colson, N. Verbeke, and **R. Kinget**
Galenical and Clinical Pharmacy, Catholic University of Leuven, Gasthuisberg, Herestraat 49, B-3000 Leuven, Belgium

Abstract

A capillary electrophoretic method with low ultraviolet (185 nm) detection is presented for the analysis of both artesunate, a hemisuccinate ester analogue of artemisinin, and succinic acid without prior derivatization. Artesunate is easily separated from its ester hydrolysis products, succinic acid and dihydroartemisinin, with the use of phosphate electrolytes at neutral pH, and this makes the method suitable for ester stability monitoring or quality control purposes. Sensitivity is shown to be strongly influenced by electrolyte and sample matrix ionic concentration ratio, which illustrates the need for careful selection of the electrolyte when direct injection of isotonic sample solutions is considered. Alkaline derivatization, which is known to generate charged compounds, is found to be useful for the analysis of neutral artemisinin derivatives, as exemplified by experiments with dihydroartemisinin.

Introduction

Qing hao, or *Artemisia annua* L., is a traditional Chinese medicinal plant used to treat malaria; however, it was not until the 1970s that qinghaosu, or artemisinin (ART), was identified as the active principle (1,2). ART is a sesquiterpene lactone with an endoperoxide group that has been shown to be essential for its antimalarial activity. As ART is only slightly soluble in water or oils and its efficacy as a drug is further hampered by a poor oral bioavailability, analogues have been prepared to overcome these problems and to improve activity. The most studied compounds have been obtained semisynthetically; they are ester or ether derivatives of dihydroartemisinin (DHA), a hemiacetal derived from ART by borohydride reduction. Artesunate (ARS) (Figure 1), obtained by esterification of succinic acid (SA) and DHA, has been reported to be highly potent and, because of its water solubility, is suitable for administration regimens in which a rapid onset of action is desirable, such as in cases of cerebral malaria. ART or its derivatives have also been used successfully in the treatment of patients with resistant malaria. This and the fact that resistance of malaria parasites toward the currently used drugs is rapidly increasing have drawn attention to artemisinin and its analogues as possible alternatives. The recent appearance of an issue of *Transactions of the Royal Society of Tropical Medicine and Hygiene* dedicated to ART has been most illustrative in this respect (3).

ART and most of its derivatives are thermolabile, lack chromophoric or fluorophoric groups, and lack functions suitable for quantitative derivatization, which precludes any straightforward analytical chromatographic method (e.g., those that would be suitable for stability studies). Several techniques have been used to address this problem. Although apparently incompatible with ART determination, gas chromatography can be used for indirect analysis of ART through its thermal degradation products (4,5). High-performance liquid chromatography (HPLC) with reductive electrochemical detection allows direct determination of ART and analogues that contain the peroxide moiety (6,7). The method, however, requires rigorous deoxygenation procedures of all reagents used and maintenance of oxygen-free analysis conditions. The peroxide function was also used for indirect chemiluminescent detection after separation by HPLC (8). Alkaline treatment of ART has been reported to generate a number of UV-absorbing degradation products (9). Consequently, various HPLC methods with either pre- or postcolumn alkaline (or acidic) derivatization have been developed; however, the former suffers from lack of specificity, as ART derivatives often generate identical products, and the latter involves a compromise between sensitivity and resolution (10–13). Recently, supercritical fluid chromatography with electron-capture detection was described for the direct analysis of ART (14).

Since its introduction in 1981, capillary electrophoresis (CE) has allowed chromatographers to achieve highly selective and efficient separations, so it has now become an established analytical separation technique that complements and, in some cases, even replaces HPLC and GC. In this paper, we report the use of CE with low UV detection for the direct determination of ARS. Because ARS carries an ionizable carboxyl group, it is well suited for CE analysis. Furthermore, because CE separa-

* Author to whom correspondence should be addressed.

tions are based on (true or apparent) differences in charge density, ARS should be well separated from its hydrolytic degradation products, DHA and SA. Inherent to the on-line optical detector design in CE is the relatively poor concentration sensitivity as compared with HPLC when using conventional UV–vis detection. The problem may be solved by using extended light path capillaries or a higher energy of the incident light beam (15). However, both the general instrumental design (capillary dimensions and on-line detector) and the composition of the separation medium (aqueous electrolyte solutions) allow for an alternative approach, that is, the use of ultrashort wavelength UV detection (down to 185 nm), thereby expanding the range of detectable compounds substantially. This feature is shown to enable direct UV detection of ARS. The importance of a number of variables relating to both sample and electrolyte composition for quantitation is demonstrated. In addition, CE after alkaline derivatization is studied as an alternative method.

Experimental

Chemicals

ARS and DHA were obtained from Mediplantex (Hanoi, Vietnam) and Profarma (Beerse, Belgium). Other chemicals used were analytical-grade SA, phosphoric acid, and potassium hydroxide (UCB; Leuven, Belgium); sodium hydroxide and tris(hydroxymethyl)aminomethane (TRIS) (Merck; Darmstadt, Germany); lithium hydroxide (Sigma; Deisenhofen, Germany); and HPLC-grade methanol (Carlo Erba; Milano, Italy). 4-(2-Hydroxyethyl)-piperazine-1-ethanesulfonic acid (HEPES) and Hanks' balanced salt solution were obtained from Gibco BRL Life Technologies (Paisley, Scotland). All compounds were used without further purification.

CE operation

Experiments were performed with a Waters Quanta 4000 CE system (Waters; Milford, MA). Detection was performed with a fixed wavelength UV detector equipped with a mercury lamp and a 185-nm filter and window. The system was operated at a constant voltage (30 kV) in the normal polarity mode, and detection was toward the cathodic end of the capillary. Fused-silica capillaries (47 cm × 50-µm i.d. or 51 cm × 75-µm i.d.) were used. When capillaries were stored overnight, they were filled with water. Each day operation was started with a vacuum purge with 0.5M NaOH followed by water. The capillary was then subjected to an electroosmotic purge after a vacuum purge with the electrolyte. All runs were preceded by a 2-min purge with the electrolyte used. Samples were introduced by gravity-induced siphoning (Δh = 10 cm; 30-s injection time). Data were collected through Waters Baseline software. Electrolytes consisted of 40mM lithium phosphate at a pH of 6.8 (unless noted otherwise) and were freshly prepared in water from a Milli-Q water purification system, filtered, and degassed immediately before use.

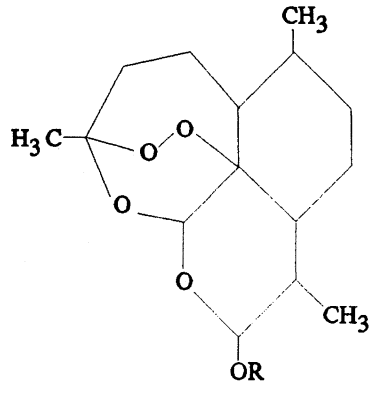

DHA R = H

ARS R = $-OC-CH_2-CH_2-COOH$

Figure 1. Structure of artesunate (ARS) and dihydroartemisinin (DHA).

Standard solutions and calibrations

Standard 10mM stock solutions of ARS or DHA were prepared in either HEPES-buffered Hanks' balanced salt solution (HBSS) or methanol and stored at –20°C. A stock solution of SA was prepared in electrolyte that was diluted 10-fold (i.e., 4mM lithium phosphate) and stored at room temperature. Calibration lines were constructed in accordance with the sample matrix composition of samples to be quantitated; more specifically, working solutions were diluted to give final sample matrix compositions of HBSS diluted threefold or electrolyte diluted 10-fold.

Derivatization

Twenty-five milliliters of KOH solution (50–1000mM) was added to 100 mL of 10mM methanolic solutions of ARS or DHA. Mixtures were allowed to react at temperatures ranging from 0°C to 80°C. Reaction was stopped at various time intervals by cooling on ice. Samples were diluted eightfold in ice-cold water immediately before analysis.

Results and Discussion

The ester bond in ARS is susceptible to hydrolysis; it produces to DHA and SA in aqueous solution. DHA is an active metabolite common to many ART analogues, so ARS can be regarded as a prodrug. However, as DHA does not possess the aqueous solubility properties of ARS, precipitates of DHA rapidly form. ARS preparations for parenteral use are therefore dispensed as the powdered drug and are to be reconstituted with sodium bicarbonate solution immediately before administration. Because it is a hemisuccinate ester, ARS has an ionizable carboxyl group, so it should be separated by CE in slightly acidic to alkaline electrolytes from both DHA and SA because of their greatly differing charge densities. CE also offers the possibility of direct sample injection, a feature of particular importance when extensive sample processing procedures may affect the stability of the compound to be measured. Because the method may be of interest not only for monitoring ester hydrolysis but also for determining ARS or its metabolic fate in in vitro experiments, ARS

was dissolved in a representative isotonic solution (i.e., HBSS) to assess possible sample matrix effects. ARS and SA show faint absorption characteristics at 200 nm or higher but can be directly imaged by UV detection at 185 nm.

In a first set of experiments, the effects of various separation conditions relating to both electrolyte and sample, as well as to instrumental parameters on separation, were studied. The reliability of ARS and SA quantitation was investigated and applied to determine temperature and pH effects on the stability of ARS in aqueous solution. Furthermore, some of the compounds proposed to have been formed after alkaline treatment of ART also carry an ionizable carboxyl group (9). Preliminary experiments were performed to assess the usefulness of this derivatization method for ARS or its active metabolite DHA, which could not be monitored by direct CE because of the absence of a charge.

Effect of electrolyte and sample matrix composition and capillary dimensions

ARS was well separated from SA in all instances with the use of sodium phosphate electrolytes with a pH of 5.6–7.6. The electroosmotic flow velocity increased with increasing pH, speeding up the migration of all analytes as shown in Figure 2. Peak shape also greatly improved with increasing pH, as could be observed by the rise in the peak height to width ratios (data not shown). HEPES, the buffering constituent present in the HBSS solvent, may interfere with the anionic analytes. Although HEPES, being a zwitterionic agent and therefore dependent on the pH for its charge, did not have any electrophoretic mobility at pH 5.6–6, the sulfonate function predominates in the neutral to alkaline pH region, conferring a net negative charge increasing with pH. In addition, as the electrophoretic mobility of HEPES increased with pH in a much faster way than ARS, comigration of ARS and HEPES was observed above pH 7.4. A peak generated from the sample matrix interfered with SA around pH 6, limiting the working pH interval to 6.2–7.4.

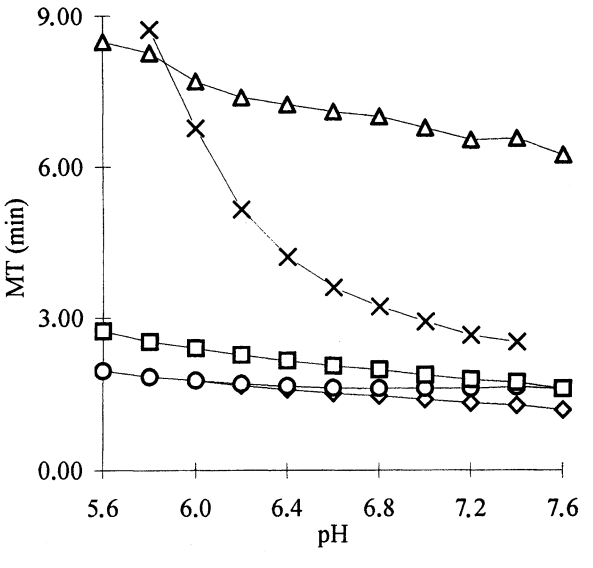

Figure 2. Effect of electrolyte pH on migration time (MT) of artesunate (ARS, □), succinic acid (SA, △), electroosmotic flow (◇), 4-(2-hydroxyethyl)-piperazine-1-ethanesulfonic acid (HEPES, O), and the interference generated by the sample matrix (X). Conditions: sample, 0.33mM ARS and 0.17mM SA in HEPES-buffered Hanks' balanced salt solution (1:3 diluted); electrolyte, 25mM sodium phosphate; capillary, 51 cm × 75-µm i.d.; applied voltage, 30 kV.

Along with pH and ionic strength, current also increased substantially. Joule heating, which develops as a result of this, may affect separation through changes in, for example, analyte dissociation, electrolyte pH, or electroosmotic flow velocity. In addition, radial temperature gradients may be generated, causing significant band broadening (16). High-conductivity electrolytes should therefore be avoided, and efficient heat dissipation should be assured. A reduction of the applied voltage was not taken into consideration because this would negatively affect migration times as well as resolution (17). The conductivity of the electrolyte could be reduced by 45% by replacing sodium hydroxide with TRIS as the neutralizing base. The use of lithium phosphate allowed a 25% reduction of the current and was preferred to the use of TRIS phosphate because of its lower background absorption. A typical electropherogram recorded under optimized conditions is given in Figure 3.

Efficient heat dissipation is more easily obtained in capillaries with smaller inner diameters because of the more favorable dissipation surface to capillary volume ratio. By further reducing the capillary diameter from 75 µm to 50 µm, an average 50% reduction of the current was observed, leaving room for the use of higher buffer concentrations. Although the use of a higher electrolyte concentration definitely caused a current increase, the important beneficial effects of improved peak shape and sample loading could be exploited. Peak height-to-width ratios increased (reflecting both a peak width decrease and height increase) with electrolyte concentration, whereas peak areas decreased, also as a result of the decreased peak widths. At comparable and acceptable currents, that is, approximately 80 µA for a 25mM lithium phosphate buffer and a 75-µm capillary versus a 40mM buffer in a 50-µm capillary, peak height-to-width ratios were comparable. The higher peak area in the wider capillary is a result of not only the longer optical path length but also a higher sample loading capacity. The injected sample volume V for hydrodynamic injection may be calculated according to Poiseuille's law for laminar flow (i.e., $V = \pi r^4 tP/8L\eta$), where r is the capillary radius, t is the injection time, P is the applied pressure, L is the capillary length, and η is the electrolyte viscosity. In this case (i.e., siphoning injection), the pressure is provided by the weight of the liquid column between the fluid levels in the sample and the cathodic electrolyte vial during injection, so $P = g\rho\Delta h$, where g is the gravitational constant, ρ is the liquid density, and Δh is the height difference. As an example, making an injection for 30 s into a capillary (47 cm × 50-µm i.d.) filled with water at 20°C with Δh = 10 cm would amount to a sample load of 9.5 nL. This corresponds to approximately 1% of the total capillary volume. In a 51-cm × 75-µm capillary, this would amount to 44 nL, which corresponds to 2% of the capillary volume.

Low sample loads may severely compromise detection, especially when the specific absorbance of the analyte is low. This is a problem that may, at least in part, be circumvented

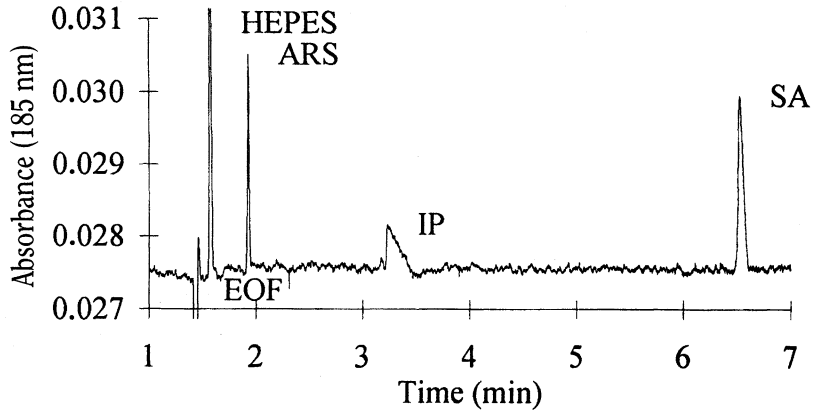

Figure 3. Electropherogram of a sample that contained artesunate (ARS) and succinic acid (SA). Conditions: sample, 0.33mM ARS–0.17mM SA in 20% HEPES-buffered Hanks' balanced salt solution; capillary, 47 cm × 50-µm i.d.; electrolyte, 40mM lithium phosphate at pH 6.8. Abbreviations: IP, sample matrix generated interference; EOF, electroosmotic flow; HEPES, 4-(2-hydroxyethyl)-piperazine-1-ethanesulfonic acid.

during electrophoresis in a process called sample stacking, which involves carefully adjusting electrolyte and sample matrix composition. If a sudden drop of solution resistivity is allowed at the sample zone–electrolyte interface, analytes in the sample zone, being subject to a higher electric field strength, rapidly migrate to the electrolyte zone where the abrupt decline in field strength also causes a sudden slowing of analyte migration. Then, a focusing phenomenon takes place at the sample–electrolyte interface. Optimized sample stacking has been reported to be possible by balancing injection time and the sample/electrolyte resistivity ratio (18). Generally, sample stacking was shown to be maximal when samples were prepared in solutions corresponding to electrolyte that was diluted 10 times.

The effect of the fraction of HBSS in the sample matrix on ARS stacking is shown in Figure 4. Although peak area is relatively unaffected by increasing sample matrix ionic concentration, the decline in peak height-to-width ratio clearly illustrates a loss of stacking and even an enlargement of the ARS zone compared with the injected sample zone. As expected, peak shape deteriorates much faster in the less concentrated electrolyte, whereas peak width increased by 50% when a 40mM lithium phosphate buffer was used with a 50-µm capillary and when the concentration of HBSS in the sample matrix was changed from 10 to 98%, a threefold increase was observed in the 25mM buffer–75-µm capillary combination. Peak heights decreased by 50% and 75%, respectively. Consequently, when ARS is analyzed in isotonic buffer solutions and concentrations are expected to near the detection limit, a narrower capillary (which allows the use of higher electrolyte concentrations and consequently less dilution of the sample) may provide superior detection in spite of the longer optical path length of the wider capillaries.

Linear dynamic range and reproducibility of ARS and SA migration time and quantitation

ARS and SA peak areas showed linearity over a concentration range from 10µM to 10mM and from 5µM to 5mM, respectively (r = .9996 for both ART and SA). Peak heights rapidly diverged from linearity with concentration, paralleling the peak shape deterioration. Detection limits were 25µM ARS and 15µM SA (30-s injection time; signal-to-noise ratio of 3), which corresponded to absolute amounts of approximately 250 and 100 fmol. Intraday and interday precision of CE analyses of ARS and SA were determined as shown in Table I. Injection times may be increased—providing higher sample loads—with the use of dilute electrolyte solutions as sample matrix. Under these conditions, the sample stacking process may be a major contributing factor in achieving a considerable enhancement of sensitivity.

Stability of ARS in aqueous solution: effect of temperature and pH

Aqueous solutions of ARS are known to be unstable; rapid hydrolysis of the ester bond and precipitation of DHA occurs. Although ester hydrolysis may obviously be monitored through the decline of the parent compound, a positive identification of the hydrolysis products and their quantitation are also frequently used. In addition to its lack of chromophoric groups, DHA does not have a permanent or inducible charge, and thus, it presents a problem when CE is used. Micellar electrokinetic capillary chromatography has, in many instances, allowed highly selective and efficient separations of neutral compounds, but its combination with indirect UV or fluorescence detection, which would be required for de-

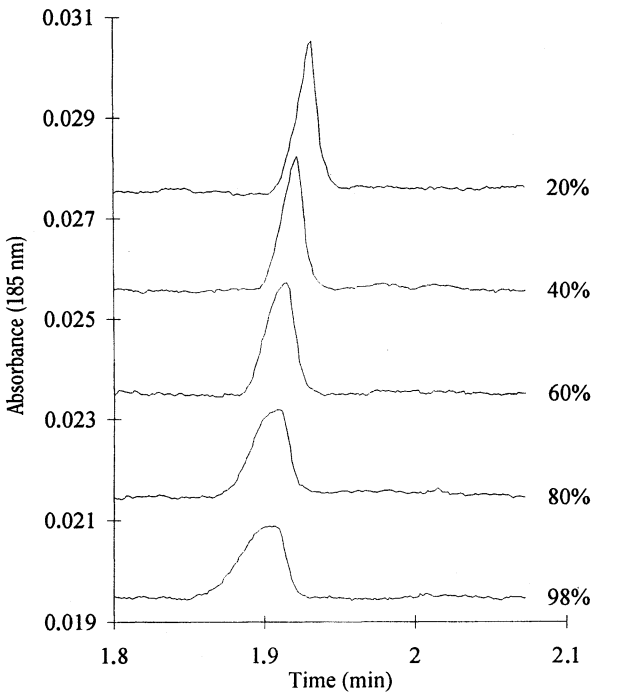

Figure 4. Electropherograms displaying the effect of sample matrix ionic concentration (% HEPES-buffered Hanks' balanced salt solution [HBSS]) on artesunate (ARS) peak shape. Conditions: sample, 0.33mM ARS in HBSS; capillary, 47 cm × 50-µm i.d.; electrolyte, 40mM lithium phosphate at pH 6.8.

tection of DHA, has not been extensively studied (19). This may be due to the fact that indirect detection techniques are generally less sensitive than their direct counterparts. However, when neither sample size nor sample concentration are limiting factors, this can hardly be regarded as an obstacle. Because ARS ester hydrolysis also yields SA, which was easily and simultaneously determined with ARS, this approach provided an alternative method of determining ARS ester stability. As an example of a possible application, the stability of aqueous ARS solutions at different temperatures was determined through quantitation of ARS and SA. ARS, dissolved in a 4mM lithium phosphate buffer at pH 7, was shown to be stable for at least 1 day when stored at 0°C: No decline in ARS was observed nor was the appearance of SA observed. At 21°C and 37°C, declines of 6% and 39%, respectively, of ARS concentration were observed after an 8-h period. The declines increased to 17% and 77%, respectively, after 1 day. An analogous experiment that varied pH of the aqueous solution (pH ranging from 5.6 to 8.3; experiment performed at 25°C) revealed no substantial differences. An average 25% decline was observed after 24 h, and only 20% of the original concentration could be detected after 1 week. The increasing SA concentration matched the disappearance of ARS, proving the equivalence of both approaches.

Table I. Intraday and Interday Reproducibility of ARS and SA Migration Times (MT), Quantitation, and Calibration Lines*

		Added	MT ART		Experimental (µm)		
		(µM)	Mean	RSD (%)	Mean	RSD (%)	*n*
Intraday	ARS	25	1.8	0.1	31	5.6	9
		133	1.8	0.2	119	3.0	9
		333	1.8	0.3	307	0.5	
	SA	25	5.4	0.4	23	2.7	9
		100	5.3	0.4	97	2.5	9
		500	5.2	0.5	497	0.6	9
Interday	ARS	25	1.8	2.5	33	3.1	6
		133	1.81	2.4	123	1.9	6
		333	1.81	2.4	315	1.8	6
	SA	15	5.6	3.0	14	14.4	11
		100	5.5	2.9	100	2.0	11
		250	5.4	3.1	250	0.8	11

* The electrolyte was 40mM lithium phosphate (pH 6.8). The capillary column was 47 cm × 50 µm. ARS samples in HBSS (diluted three times). SA samples in electrolyte (diluted ten times).

Alkaline derivatization of ARS and DHA: effect of base concentration, reaction temperature, and time

One of the most frequently used methods for the determination of ART and its derivatives is HPLC with pre- or post-column alkaline treatment, which allows UV detection of the degradation products. The applicability of this derivatization method before analysis by CE was investigated because some of the compounds proposed to have been formed after alkaline treatment of ART carry an ionizable carboxyl group (9). This should also be important for the analysis of the neutral compound DHA. In addition to ester hydrolysis, alkaline treatment decomposed ARS into a number of compounds that could be separated by CE, confirming a previous report in which at least five degradation products could be discerned (10).

The extent and the rate of transformation were highly dependent on both the concentration of the base and the reaction temperature. At low KOH concentrations (0.05M) little if any degradation was observed, even at 60°C (Figure 5, lower trace). When the KOH concentration was increasd to 0.5M, ARS was completely converted (within 1 min at room temperature) to a derivative with higher mobility (derivative 1). An SA peak was present but did not account for the complete breakdown of ARS, suggesting derivative 1 to be still associated with SA and therefore an intermediate specific to ARS. This could be confirmed by running parallel derivatization experiments on DHA. In no instance could derivative 1 be detected. When the temperature was raised to 40°C or 60°C, a second derivative (derivative 2) appeared at the expense of derivative 1, while SA concentration also rose (Figure 5, top trace). At 1M

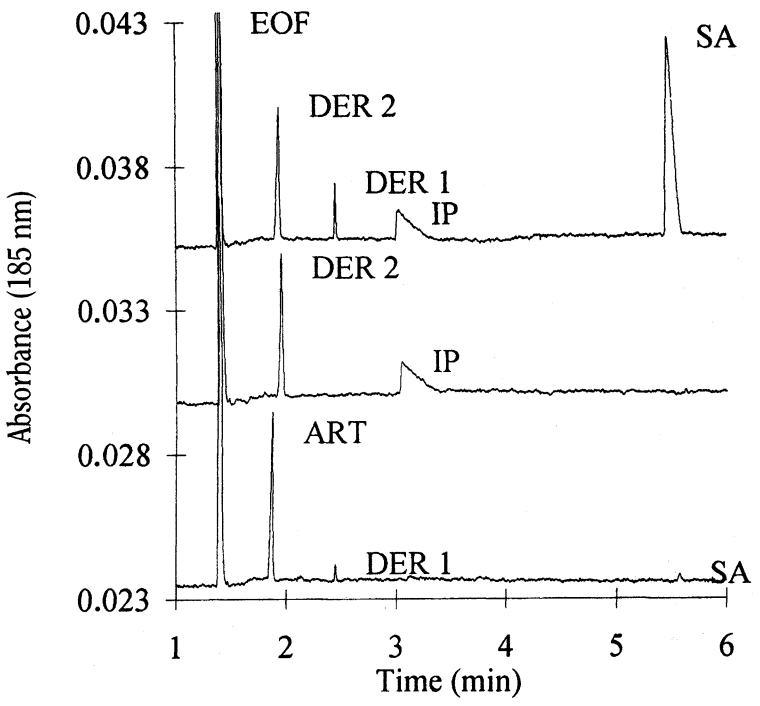

Figure 5. Electropherogram of alkaline-derivatized artesunate and dihydroartemisinin. Derivatization conditions: 15 min at 60°C of artemisinin (ART) with (bottom trace) 0.05M or (top trace) 0.5M KOH and (middle trace) DHA with 0.5M KOH; capillary, 47 cm × 50-µm i.d.; electrolyte, 40mM lithium phosphate at pH 6.8. Abbreviations: DER 1 and DER 2, first and second derivatives formed; SA, succinic acid; IP, sample matrix generated interference; EOF, electroosmotic flow.

KOH and 80°C, derivative 1 was only short-lived and the formation of derivative 2 paralleled the appearance of SA. Within 10 min, complete conversion was reached, which was estimated through the equimolar presence of SA compared with starting ARS concentration, and the attainment of the plateau, which was apparent for both SA and derivative 2. The amount and the time course of derivative 2 formation in DHA experiments yielded almost identical results. Derivative 2 has a slightly higher mobility than ARS, which might be expected if it proved to be identical to the major compound reported to be formed by alkaline treatment of ART; its formation involves ring opening and rearrangement, leaving a compound with the same molecular weight and a carboxyl group and, consequently, a slightly higher charge density than that of ARS.

Although Zeng and Li (9) reported a better than 88% conversion rate, they found that a number of minor compounds were also formed. A closer examination of the derivative 2 peak revealed that it first actually appeared as a peak cluster composed of at least three different closely migrating compounds whose ratio changed as the reaction proceeded. After a 1-h reaction time at 80°C, two peaks remained with a peak-area ratio of approximately 2:8. At the pH of the CE electrolyte (i.e., pH 6.8), the derivatization mixture showed an absorption maximum at 235 nm, allowing detection at higher wavelengths. Although multiple product formation does not simplify quantitation, alkaline derivatization of ART or its derivatives, whether performed pre- or postcolumn, has proved to be satisfactory in HPLC. Although a moderate 25% gain in sensitivity was observed for ARS at 185 nm, derivatization clearly is a prerequisite for DHA analysis by CE. The results obtained with DHA suggest that the method may also be applicable to other neutral ART analogues.

Conclusion

CE offers sufficient sensitivity for the quality control of ARS preparations without elaborate sample preparation. However, it may not provide the concentration sensitivity needed for the analysis of samples from pharmacokinetic studies. The low sample consumption of CE and the high sensitivity to absolute amounts are definitely an advantage in this respect, but extensive sample volume reduction will still be needed. In addition, it was shown that the sample matrix may be particularly important for sensitivity. Alkalinization extended the method to the determination of neutral ART analogues.

Acknowledgment

Mrs. Ngo Thu Hoa (College of Pharmacy, Hanoi, Vietnam) is gratefully acknowledged for providing us with artesunate.

References

1. D. Klayman. Qinghaosu (artemisinin): an antimalarial drug from China. *Science* **228:** 1049–55 (1985).
2. X. Luo and C. Shen. The chemistry, pharmacology, and clinical applications of qinghaosu (artemisinin) and its derivatives. *Med. Res. Rev.* **7:** 29–52 (1987).
3. *Trans. Royal Soc. Trop. Med. Hyg.* **88 (Suppl 1):** (1994).
4. A. Theoharides, M. Smyth, R. Ashmore, J. Halverson, Z. Zhou, W. Ridder, and A. Lin. Determination of dihydroqinghaosu in blood by pyrolysis gas chromatography/mass spectrometry. *Anal. Chem.* **60:** 115–20 (1988).
5. J. Ferreira, D. Charles, K. Wood, J. Janick, and J. Simon. A comparison of gas chromatography and high performance liquid chromatography for artemisinin analyses. *Phytochem. Anal.* **5:** 116–20 (1994).
6. V. Melendez, J. Peggins, T. Brewer, and A. Theoharides. Determination of the antimalarial arteether and its deethylated metabolite dihydroartemisinin in plasma by high performance liquid chromatography with reductive electrochemical detection. *J. Pharm. Sci.* **80:** 132–38 (1991).
7. Z. Zhou, J. Anders, H. Chung, and A. Theoharides. Analysis of artesunic acid and dihydroqinghaosu in blood by high performance liquid chromatography with reductive electrochemical detection. *J. Chromatogr.* **414:** 77–90 (1987).
8. M. Green, D. Mount, G. Todd, and A. Capomacchia. Chemiluminescent detection of artemisinin—Novel endoperoxide analysis using luminol without hydrogen peroxide. *J. Chromatogr. A.* **695:** 237–42 (1995).
9. M.-Y. Zeng and L.-N. Li. Chemical transformations of Qinghaosu, a peroxide antimalarial. *Tetrahedron.* **39:** 2941–46 (1983).
10. P. Edlund, D. Westerlund, J. Carlqvist, B. Wu, and Y. Jin. Determination of artesunate and dihydroartemisinin in plasma by liquid chromatography with post-column derivatization and UV-detection. *Acta Pharm. Suec.* **21:** 223–34 (1984).
11. H. ElSohly, E. Croom, and M. ElSohly. Analysis of the antimalarial sesquiterpene artemisinin in *Artemisia annua* by high-performance liquid chromatography (HPLC) with postcolumn derivatization and ultraviolet detection. *Pharm. Res.* **4:** 258–60 (1987).
12. O. Idowu, G. Edwards, S. Ward, M. Orme, and A. Breckenridge. Determination of arteether in blood plasma by high-performance liquid chromatography with ultraviolet detection after hydrolysis with acid. *J. Chromatogr.* **493:** 125–36 (1989).
13. S. Zhao and M.-Y. Zeng. Application of precolumn reaction to high-performance liquid chromatography of Qinghaosu in animal plasma. *Anal. Chem.* **58:** 289–92 (1986).
14. D. Mount, G. Todd, and V. Navaratnam. Packed-column supercritical fluid chromatography of artemisinin (qinghaosu) with electron-capture detection. *J. Chromatogr. B.* **666:** 183–87 (1995).
15. M. Albin, P. Grossman, and S. Moring. Sensitivity enhancement for capillary electrophoresis. *Anal. Chem.* **65:** A489–97 (1993).
16. J. Knox. Thermal effects and band spreading in capillary electroseparation. *Chromatographia* **26:** 329–37 (1988).
17. J. Jorgenson and K. Lukacs. Zone electrophoresis in open-tubular glass capillaries. *Anal. Chem.* **53:** 1298–1302 (1981).
18. D. Burgi and R.-L. Chien. Optimization in sample stacking for high-performance capillary electrophoresis. *Anal. Chem.* **63:** 2042–47 (1991).
19. J. Vindevogel and P. Sandra. *Introduction to Micellar Electrokinetic Chromatography.* Hüthig, Heidelberg, Germany, 1992, pp 121–22.

Manuscript accepted January 23, 1996.